Optimization of Process Planning for Reducing Material Waste in Extrusion Based Additive Manufacturing

Jingchao Jiang, Xun Xu, Jonathan Stringer

Department of Mechanical Engineering, University of Auckland, New Zealand

Abstract

Among the available additive manufacturing technologies, extrusion based 3D printing (otherwise known as fused deposition modelling or fused filament fabrication) is among the most commonly used due to low cost and relative simplicity. However, such printers still suffer from redundant support material waste (both interior and exterior) when printing large-volume solid objects or objects with overhangs. The support material can also be a significant cause of long part production time and higher energy consumption during manufacture. Hence, we propose a new support generation strategy considering both interior and exterior support via AM process planning to reduce the total amount of material consumption, production time and energy consumed for manufacturing an object. Print path and print orientation are both considered as significant factors and are both optimized for achieving the lowest consumption of material. The areas to be filled on each layer are determined according to the printable threshold overhang angle (PTOA) and the longest printable bridge length (LPBL). The characteristics of LPBL and PTOA are fully considered for saving more material. Several tests are used to verify the proposed strategy and the results show that this strategy can considerably reduce material waste, production time and energy consumed compared with conventional strategies, enabling AM to be a more environmentally friendly and sustainable manufacturing technique.

Keywords: Additive manufacturing; Longest printable bridge length; Printable threshold overhang angle; Support.

**Corresponding author: Jingchao Jiang, Department of Mechanical Engineering, University of Auckland, New Zealand. Email: jjia547@aucklanduni.ac.nz*

1. Introduction

Additive manufacturing (AM) is defined by the joint ISO/ASTM terminology standard to be the "process of joining materials to make parts from 3D model data, usually layer upon layer, as opposed to subtractive manufacturing and formative manufacturing methodologies" [1]. The salient part of the definition is use of a computer to translate a solid model into a real part. The technologies represented by AM are the 3D analogue to ubiquitous 2D printers. This similarity of AM to 2D printing has given rise to the alternate common name of 3D printing. 3D printing technologies have been rapidly developed and widely applied in the fields of engineering, medicine and personalized production [2,3]. Among these technologies, extrusion based 3D printers (fused deposition modelling, FDM, or fused filament fabrication, FFF) are amongst the most popular because of their low cost and simplicity.

Currently, much research has been carried out to reduce the environmental impact induced by AM [4,5]. Though AM can be considered more environmentally-friendly than conventional subtractive manufacturing in terms of material usage, it can be made still more sustainable by improving process planning and design. A design of experiments approach was launched by Griffiths et al. [6] for minimizing energy and waste during the production of parts manufactured by 3D printing. Material and energy loss due to human and machine error in commercial FDM printers was investigated by Song and Telenko [7]. Another important factor influencing sustainability of AM is support material waste (both interior and exterior). The printing process of FDM starts from the bottom of a product and continues successively layer by layer to the top [8–11]. As a consequence, each layer can only be deposited on top of an existing surface, otherwise the print material falls due to gravity before solidification, resulting in a structure different from that desired [12]. This leads to problems for overhangs that cannot be printed as there is no supporting layer beneath them [13–15]. Therefore, sacrificial external support structures are needed for assisting overhanging features in 3D printing processes. Also, this means every layer needs to have material beneath it, even for the inside of an object. Alternatively, multi-axis systems have been investigated to achieve support-free fabrication with a relatively high associated equipment cost [16,17]. For parts that do not have significant mechanical need for interior material (e.g. for rigidity), the interior regions do not need to be filled because they have no effect on part geometry and material can be saved accordingly. Both interior and exterior support structures can be viewed as undesirable structures that are fabricated alongside the object. After fabrication completes, external supports are chemically

or mechanically removed and discarded, thus wasting the material used. This usually involves human intervention and therefore is time-consuming and expensive.

AM print orientation plays an important role in AM processes, which could significantly influence the usage of support. Altering the orientation of the supported parts for minimizing support volume has been investigated by [18–22]. However, all the above studies focused on exterior support optimization rather than inner infill of objects. Little attention has been paid to optimizing inner infill structures to save more materials besides the following [23–25]. Lu et al. [25] utilized the Voronoi diagram to compute irregular honeycomb-like volume tessellations which define the inner structure. They used a honeycomb-cell structure as inner support based on a hollowing optimization algorithm. Jin, Du and He [23] optimized the inner structure based on input contours and the self-supporting capability of material. Lee et al. [24,26] proposed a block-based inner support structure generation algorithm for saving infill material. In this paper, a new support generation strategy by optimizing AM process planning is proposed for saving both interior and exterior support usage. Process planning plays the role as a bridge between AM machines and virtual models by transferring the models into codes that can guide and control the hardware. The process planning of different AM techniques usually has similar procedures and mainly can be divided into four stages: print orientation determination, support generation, slicing and path planning. Each stage will have effects on material use, print time and finished quality from different aspects. Fig. 1 shows an illustration of process planning in AM processes. The print orientation means the location and direction of the part to be sliced and deposited. Besides the influence on the number of sliced layers and print time, a suitable print orientation can also save a lot of interior support material that is considered as a factor in this paper and will be detailed in the following sections. Based on the determined orientation, overhangs are recognized to generate support structures that would be removed in the post-processing phase. The slicing stage converts the 3D model into a series of layers for 3D fabrication. This may come before or after support generation, depending on the chosen support generation methods. The stage of path generation means creating the print path corresponding to the previously obtained layer for manufacturing a part. This usually comes after the support is generated. However, in this paper, print path is considered as an important factor of interior and exterior support usage and thus is considered before support generation to improve manufacturing efficiency and manufacturing time.

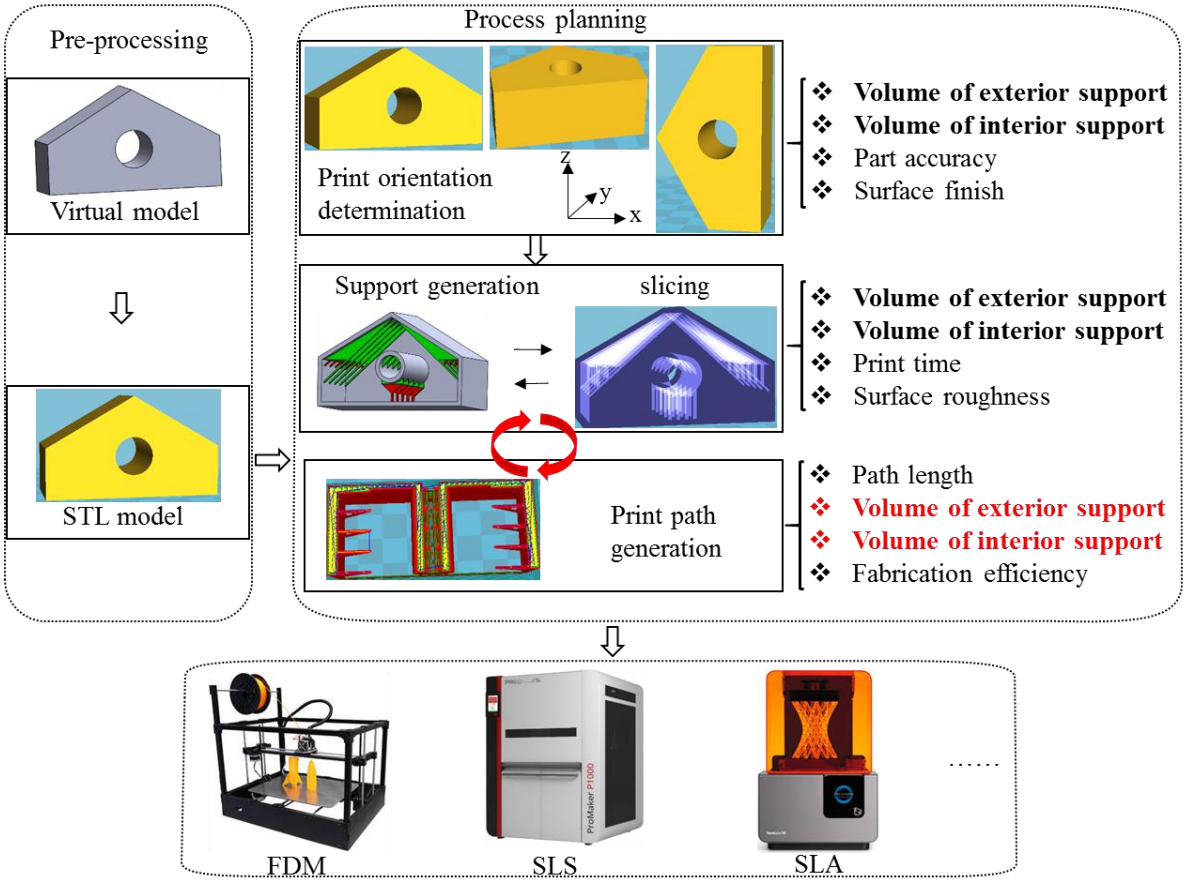

Fig. 1 An illustration of process planning in AM processes

The structure of this paper is arranged as follows. In Section 2, the concepts of longest printable bridge length (LPBL) and printable threshold overhang angle (PTOA) are introduced first, as well as their effect on support usage. Section 3 illustrates the procedure of five steps for generating support based on LPBL and PTOA. The effect of process planning (i.e. print orientation and print path) on support material consumption is displayed in section 4, as well as an optimal print strategy selection algorithm. Experimental demonstration and some discussions are shown in section 5. The last section ends the paper with some conclusions.

2. Effect of PTOA and LPBL on support consumption

For easier understanding of the proposed support optimization strategy, background on printable threshold overhang angle (PTOA) and longest printable bridge length (LPBL) are introduced first, as well as their impact on support consumption.

2.1. PTOA

Due to the layer-by layer nature of 3D printing, every deposited layer must have some kind of preceding layer deposited beneath it to support the new layer against gravity. A possible

exception to this is overhangs, which can sometimes be fabricated without support layers when the overhang angle is larger than some threshold. PTOA means an overhang with the lowest angle that can be fabricated without adding support during the deposition process. In this paper, the overhang angle (β) is defined as the angle between the x-y plane and the overhang surface tangent in the x-z (or y-z) plane (see Fig. 2). Generally, PTOA is set at 45° in most printers. Some also take a test first to determine the angle size as it may be different according to printers and materials [24,27,28]. Also, print process parameters are influential to PTOA according to our previous research [29]. Fig. 3 shows some printed overhangs in different angle sizes with the smallest printable size (the cross-section in the x-y plane is a square of 0.8×0.8 mm). As the aim of PTOA test in this study is for support, the surface quality of the printed overhang pillars is not the focus, once the overhang pillar in the smallest printable size is able to be self-supported, the corresponding overhang angle size is the PTOA. In this paper, the characteristics of PTOA is fully considered for minimizing support usage.

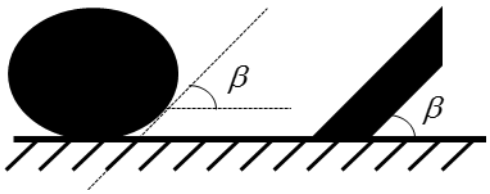

Fig. 2 Definition of overhang angle (β) in this paper

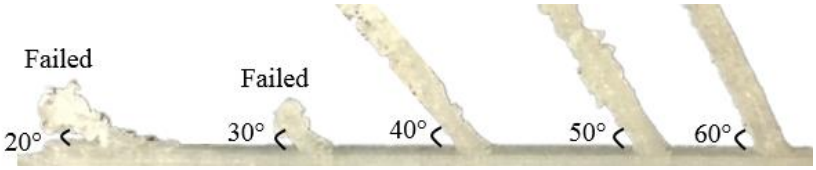

Fig. 3 Printed overhangs in different overhang angle sizes

Fig. 4 shows a simple example on the optimization of a cylinder. The solid part is shelled and hollowed firstly based on the requirement of the wall thickness. The general inner infill is the whole interior of the cylinder which is filled with relatively sparse structures without any optimization as shown in Fig. 4(a). By contrast, the inner volume to be filled can be optimized by modifying its inner topology by fully considering PTOA as shown in Fig. 4(b). It should be noticed that the inclination angle of the generated internal surface cannot go beyond the PTOA. As can be seen from Fig. 4, the fabrication of the modified part would reduce material consumption, while maintaining the same external geometry. With the modified internal topology, the part itself can be fabricated smoothly without any other additional structures in the internal space due to the consideration of PTOA. This strategy can also be used for exterior support generation.

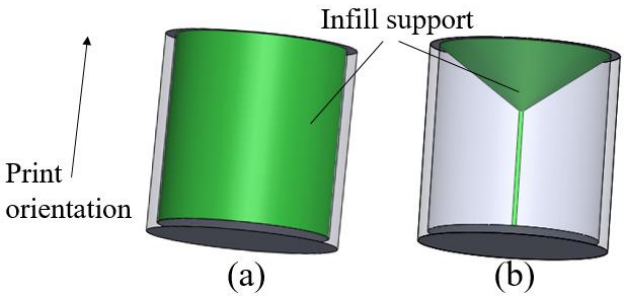

Fig. 4 (a) General inner infill; (b) Optimized infill considering PTOA

2.2. LPBL

LPBL means the bridge of longest length a 3D printer can print (with satisfactory dimensional tolerance and surface finish) without support structure underneath it. During a printing process, there are many factors (e.g. print temperature, print speed, solidification speed) that may influence LPBL. Fig. 5 shows some printed bridges with different lengths under different process parameters and the same print path direction. It clearly shows that LPBL can be achieved in various lengths when changing process parameters. At the same time, the characteristics (e.g. strength, solidity, surface quality) of printed part can also be influenced by these process parameters [30,31]. For satisfying the requirements of a product, the process parameters will need to be in a certain range. Our previous work shows more details of LPBL [32]. The satisfied LPBL can be experimentally tested according to the required process parameters. In this paper, LPBL will be integrated into our proposed support strategy for reducing material consumption.

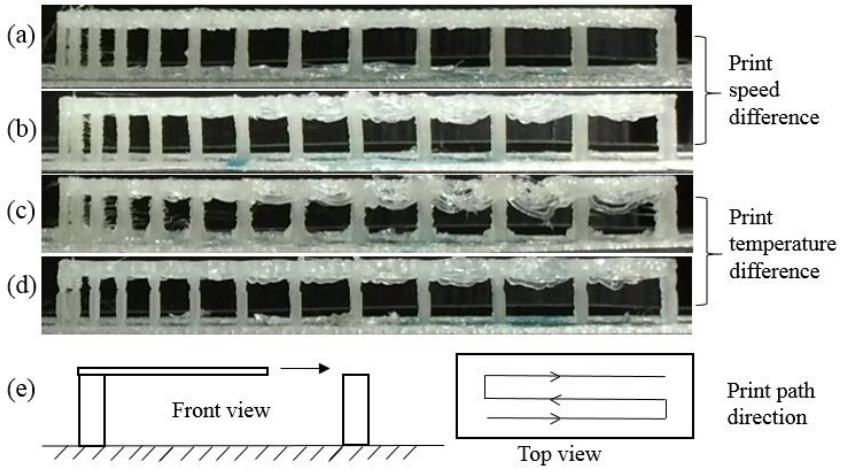

Fig. 5 Samples printed in different conditions; (a) Part printed in print speed of 5 mm/s, cooling fan speed of 250 RPM, print temperature of 190 ℃; (b) Part printed in print speed of 95 mm/s, cooling fan speed of 250 RPM, print temperature of 190 ℃; (c) Part printed in print temperature of 220 ℃, cooling fan speed of 250 RPM, print speed of 35 mm/s; (d) Part printed in print temperature of 175 ℃,cooling fan speed of 250 RPM, print speed of 35 mm/s; (e) Print path illustration [32]

For a specific layer, the areas to be filled can be achieved through a number of different print path strategies. Generally, most 3D printing processes use two patterns for generating print path: the direction-parallel method and the contour method, as shown in Fig. 6. As can be imagined, the support usage may change when altering print path strategy since the supports of a bridge need to be perpendicular to the print path based on LPBL. Fig. 7 shows a sample part with two print path strategies and their corresponding generated supports. The support (green) volume is liable to vary in different print path strategies.

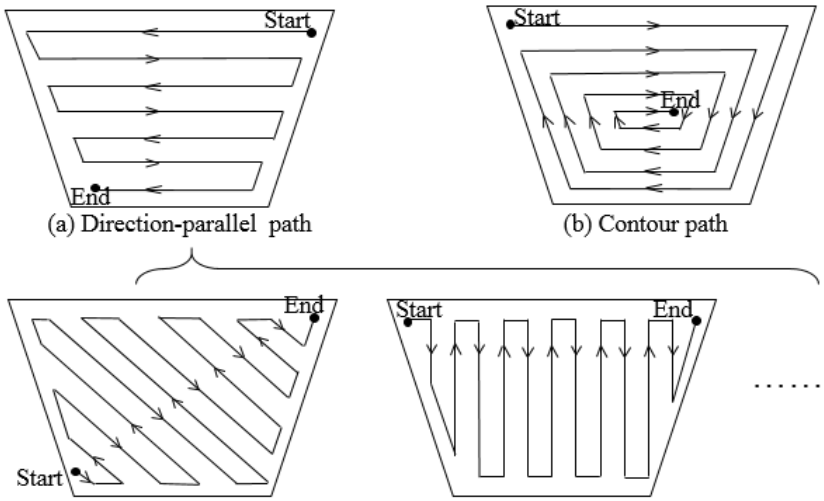

Fig. 6 Two general path patterns (Start point and end point can be changed)

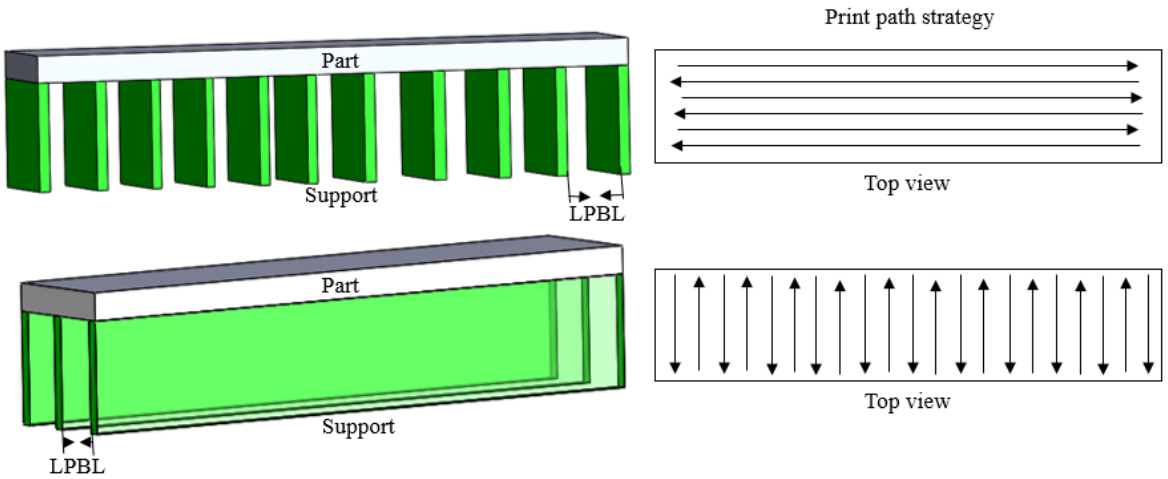

Fig. 7 Different support usages in two print path strategies based on LPBL

3. Generating supports based on the LPBL and PTOA

In the previous section, LPBL, PTOA and their impact on support usage have been introduced. Based on this background, a support generation strategy that fully takes advantage of LPBL and PTOA is proposed as the following five steps. The illustration of these five steps use an

example part shown in Fig. 8. For easier visualisation of the interior support, all the front faces of parts in the figures have been made transparent.

Step 1: Set print orientation as shown in step 1 of Fig. 8.

Step 2: Set print path strategy as shown in step 2 of Fig. 8.

Step 3: Detect areas that need support after shelling and hollowing the part based on wall thickness requirement. All overhang features will need support when the overhang angle is lower than PTOA. Mark these areas as Area(support).

Step 4: Support generation by fully considering PTOA and LPBL.

In this step, support will be generated based on the longest LPBL and PTOA as shown in step 4 of Fig. 8. First, generate the support of level 1 (green struts in this figure) on Area(support) based on PTOA. Second, generate support of level 2 (red struts) based on the longest LPBL according to corresponding print path direction. The created support of level 2 should be perpendicular to the print path for assisting support of level 1. Set LPBL as t. Then, the rule for generating support of level 2 is creating struts every t distance until the distance between the last strut and the end point is equal or less than t. For area A in step 4 of Fig. 8, the rule for choosing d_1 or d_2 for support is based on the "shortest" criterion. After obtaining the point where $d_1 = d_2$, the area on the left hand side will use wall-based struts based on PTOA while the area on the right hand side will use struts perpendicular to l_0 with the aim of consuming the least material. As PTOA is generally less than 45°, this makes all the red struts perpendicular to l_0 have an overhang angle size larger than 45°. This means all the red struts can be self-supported while having the shortest strut length when they are perpendicular to l_0. For area B in step 4 of Fig. 8, the rule for generating support is also based on the "shortest" criterion by fully considering PTOA and LPBL.

Step 5: Generate final supports.

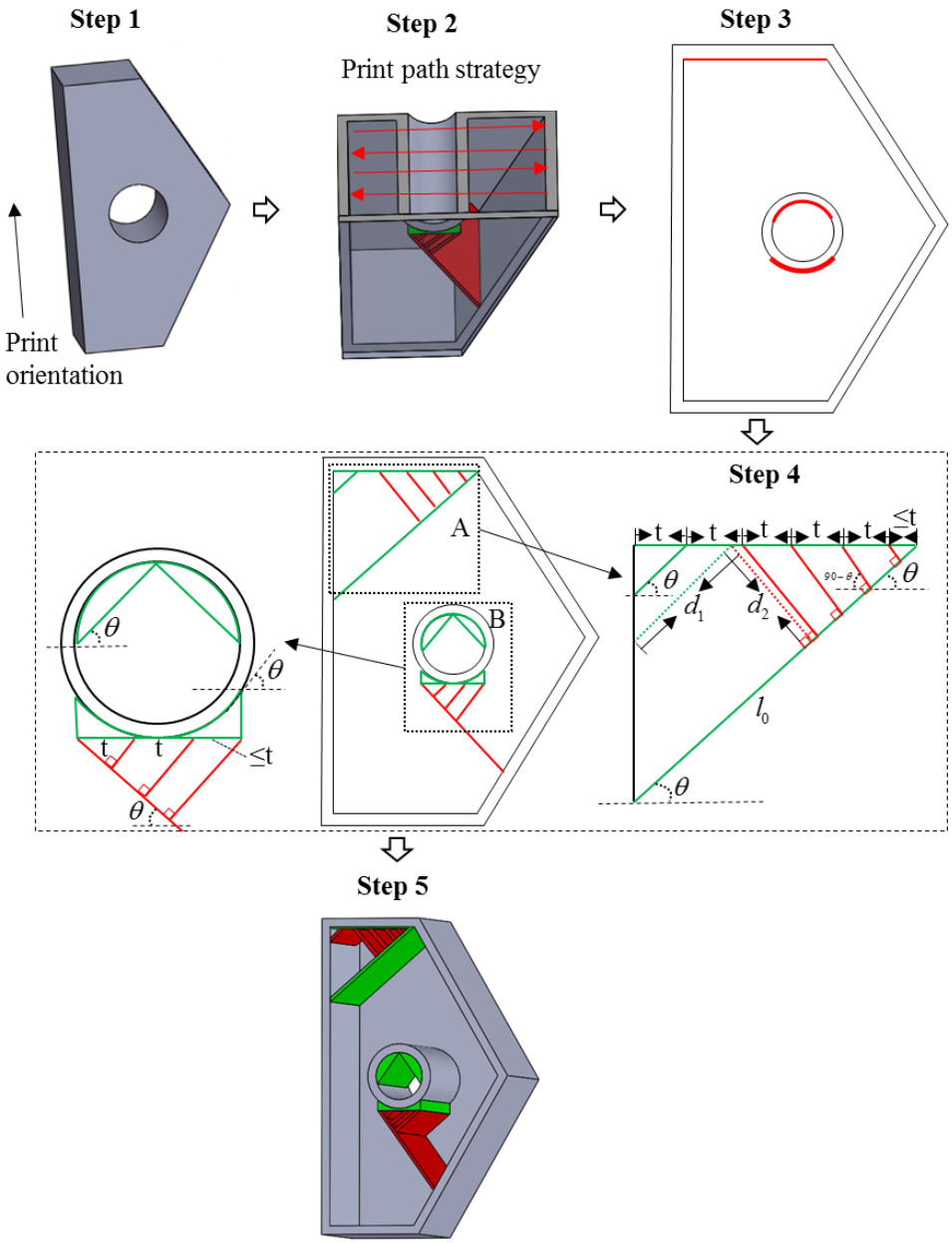

Fig. 8 Procedure of generating support based on LPBL and PTOA

4. Process planning for further reducing support usage

Once the procedure for generating support based on LPBL and PTOA is established, further process planning is also necessary to reduce the support usage, as different print path strategies and print orientations will make a significant contribution. The effects of process planning on support consumption will be illustrated in this section.

4.1. Effect of print path strategy

Print path is a significant factor in support consumption as the supports based on LPBL have to be perpendicular to the print path to fully take advantage of LPBL. Fig. 9 shows generated supports in different print path strategies on the same part.

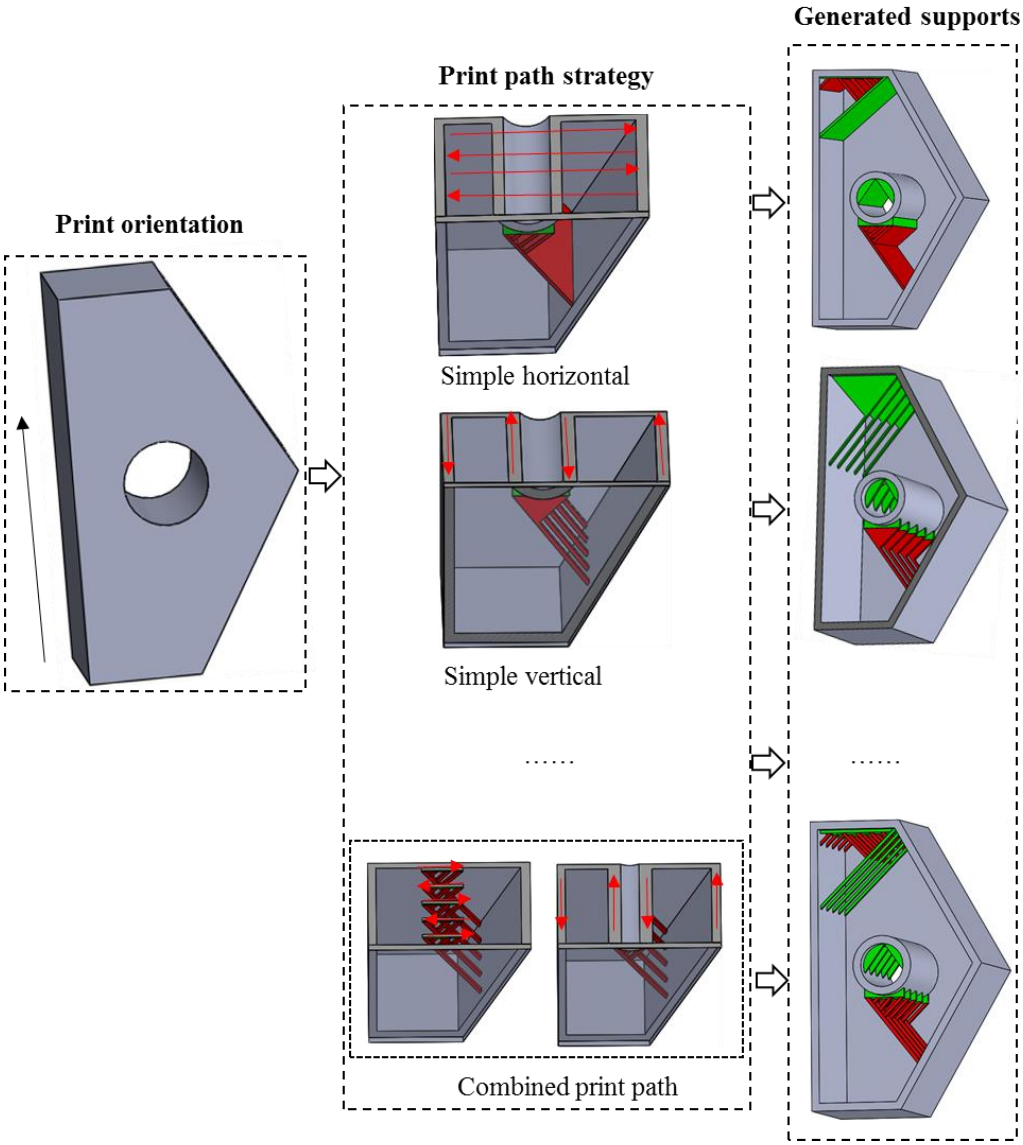

Fig. 9 Generated supports in different print path strategies

As can be seen, support volume is quite different in different print path strategies when print orientation and other print parameters are the same. For this object in this print orientation, it is easy to distinguish that the combined print path strategy is the most economical. The exact support usage volume of this strategy can be calculated as follows when the dimensions of this object are as shown in Fig. 10.

The support volume in area A of Fig. 10(a) can be calculated as follows,

$$V_A = (\sum_{1}^{n} l_i + \frac{l_a}{\cos\theta} + l_a) \times (2D_{nozzle})^2 \quad (1)$$

where $n = \lceil \frac{l_a}{t} \rceil + 1$ and $2D_{nozzle}$ is the smallest printable size of an overhang pillar. D_{nozzle} is the diameter of the print nozzle. The support volume in area B and C of Fig. 10(a) can also be estimated accordingly:

$$V_B = [\frac{\theta \pi r^2}{90} - r^2 \sin(2\theta)] \times 2D_{nozzle} \quad (2)$$

$$V_C = [(R - R\cos\theta)R\sin\theta - (\frac{\theta \pi R^2}{180} - R^2 \sin\theta\cos\theta)] \times 2D_{nozzle} + (\sum_{0}^{m} h_i)(2D_{nozzle})^2 \quad (3)$$

where $m = \lceil \frac{R\sin\theta}{t} \rceil + 1$. The total support volume of each unit in x-z plane is the sum of exterior support volume (V_B) and interior support volume ($V_A + V_C$). There are $\lceil \frac{D}{t} \rceil + 1$ units as shown in Fig. 10(b). Hence the total support volume for this whole part is $V = (V_A + V_B + V_C) \times (\lceil \frac{D}{t} \rceil + 1)$. Once the support volume usage for each different print path is known, the most appropriate print path strategy for support usage (e.g. lowest support consumption) can be utilized.

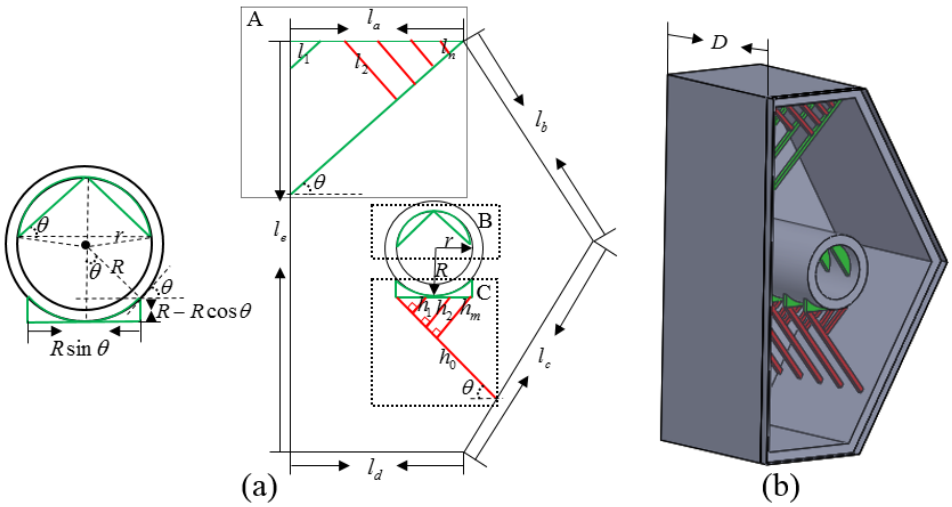

Fig. 10 Dimensions of sample object

4.2. Effect of print orientation

Print orientation is another important factor in support consumption. All the corresponding support struts will be re-set based on a new print orientation according to LPBL and PTOA.

The volume of support can be calculated accordingly as illustrated previously. Fig. 11 shows some generated supports of the same part in a different print orientation. The support volumes in Fig. 11 are different from the print orientation in Fig. 9.

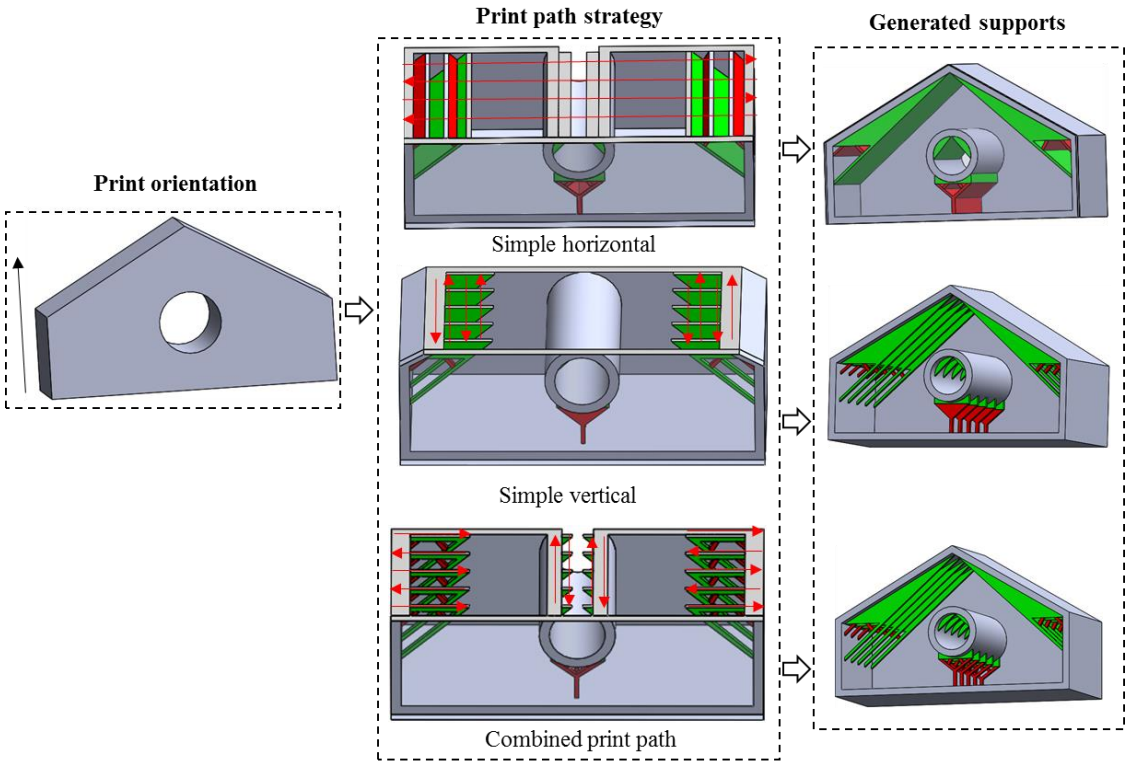

Fig. 11 Generated supports in different print path strategies under another print orientation

4.3. Obtaining the optimal print orientation and print path strategy

The algorithm for obtaining the optimal print orientation and print path is shown in Fig. 12 based on the previous illustrations. In this algorithm, *n* is the number of print orientation options and m_n is the number of print path strategies in each print orientation. The value of sum in this algorithm can be set at any value as long as it is large enough. Once the best print strategy is obtained, parts can be accordingly fabricated with the lowest material consumption.

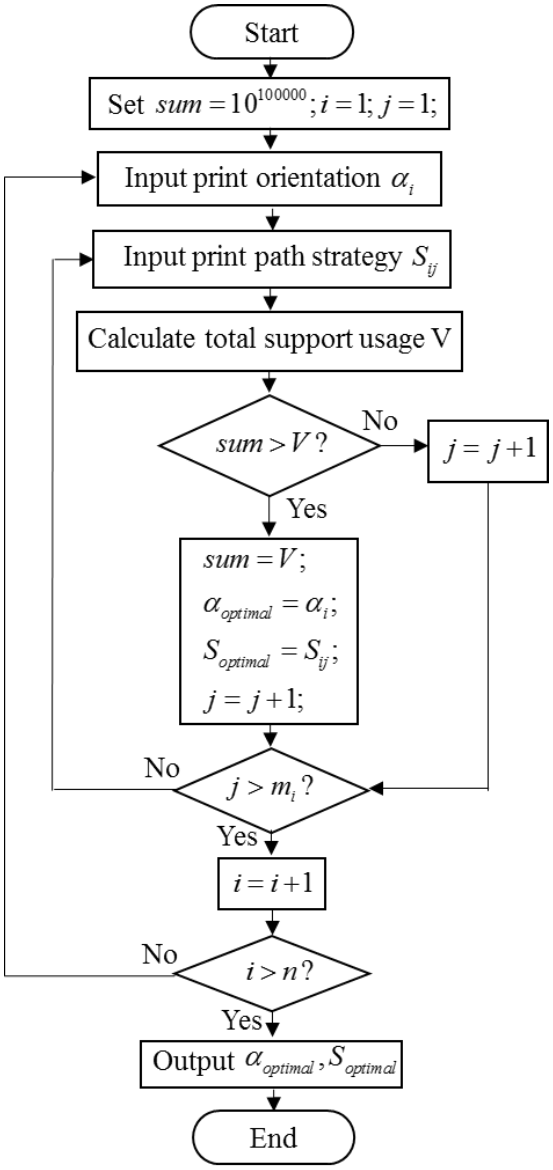

Fig. 12 Algorithm for obtaining the optimal print orientation and print path strategy

5. Demonstration and discussion

To verify the proposed support generation strategy, “U”, “O” and “A” parts were fabricated on a Kossel Delta 3D printer by using the optimized print strategy. The build area shape of the 3D printer is circular with maximum width of 180 mm, maximum depth of 180 mm and maximum height of 300 mm. The nozzle diameter of this printer is 0.4 mm. Polylactic Acid (PLA) was used for printing these parts.

Before optimizing the print strategy, the longest LPBL and PTOA are tested first with the process parameters of print temperature of 190 °C, print speed of 20 mm/s, cooling fan speed of 250 RPM and layer thickness of 0.2 mm. According to the experimental results, LPBL can be achieved at 2.0 mm with no deformation visible to the naked eye and PTOA can be achieved

at 40° under these print parameters in this Kossel Delta printer (as shown in Fig. 13). Therefore, the optimization process is carried out based on the corresponding LPBL and PTOA. Fig. 14 shows the best print strategies of these three parts and their dimensions, as well as corresponding generated supports and printed parts.

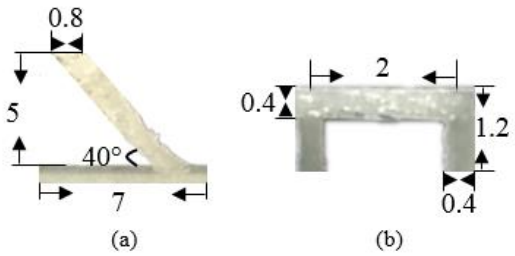

Fig. 13 Printed PTOA (a) and LPBL (b) with the process parameters of print temperature of 190 °C, print speed of 20 mm/s and cooling fan speed of 250 RPM (Unit: mm)

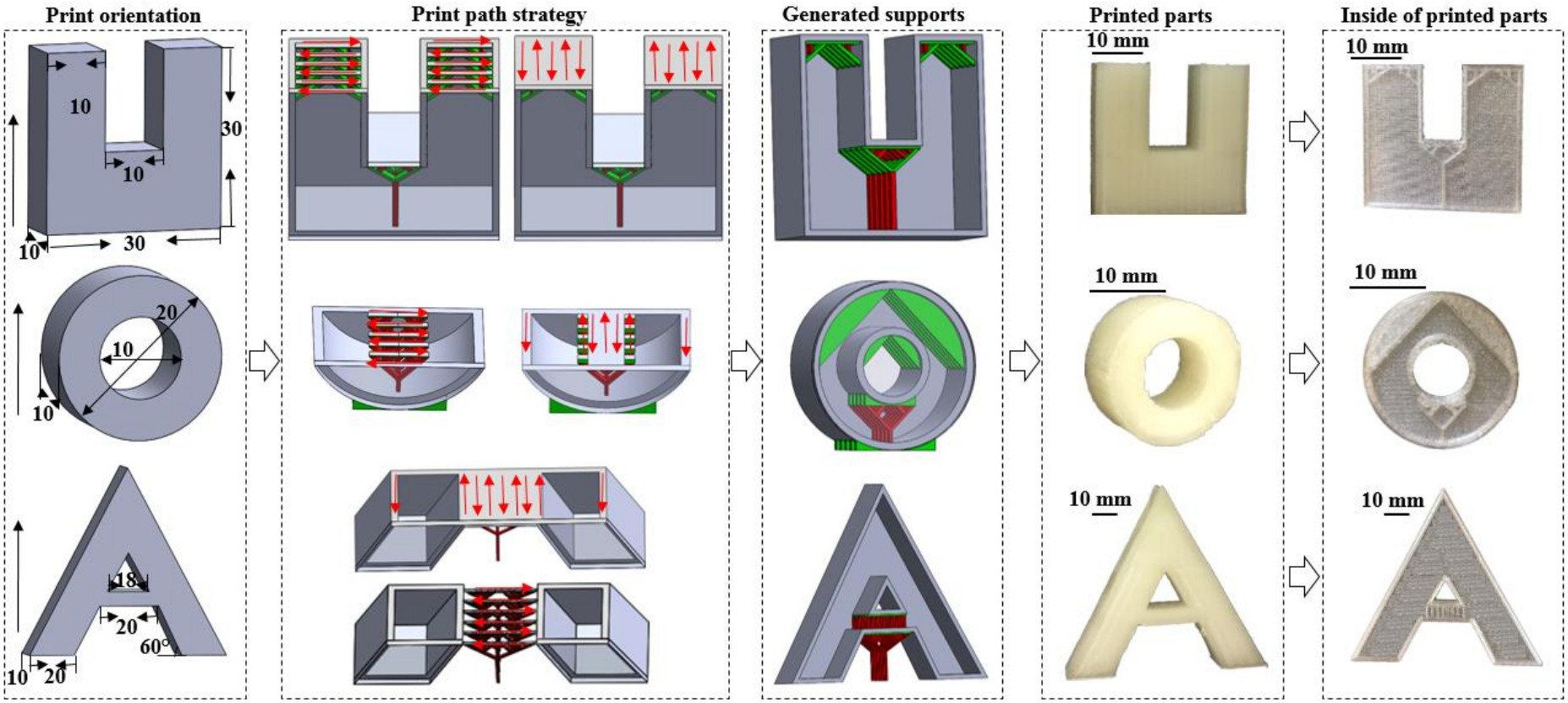

Fig. 14 Best strategies for fabricating “U”, “O” and “A” parts and their dimensions (Unit: mm), as well as corresponding generated supports and printed parts

5.1. Material consumption

For comparison with pre-existing generic support methods, the same three parts were fabricated by our strategy and conventional line support methods with infill densities of 20 %, 50 % and 80 % in the print orientation shown in Fig. 14. The wall thickness is set at 1.2 mm for shelling and hollowing and other process parameters are set as follows: print temperature of 190 ℃, print speed of 20 mm/s, cooling fan speed of 250 RPM and layer thickness of 0.2 mm. The total material consumption after experiments in different methods are shown in Table 1. As can be seen from this table, our strategy can effectively reduce the material usage. For the "O" part, the material savings can reach at 29.3 %, 39.6 % and 46.3 %, respectively. The material consumption of the "A" part can be reduced to 4.8 g by our strategy. The experimental results validate that our support strategy can significantly reduce the total material consumption by fully taking advantage of LPBL and PTOA.

Table 1 Total material consumptions in different print strategies (Unit: g)

	Our strategy	20% infill	50% infill	80% infill
"U" part	4.1	5.6	7.3	9.4
"O" part	2.9	4.1	4.8	5.4
"A" part	4.8	7.5	8.7	9.3

5.2. Production time

According to [24], the most significant amount of time during a fabricating process is consumed in manufacturing the interior support area. As the print strategy proposed in this paper can significantly reduce the interior support material consumption, it is therefore apparent that it is capable of considerably improving the manufacturing time efficiency. As can be seen from Table 2, our strategy can save at least 7.5% of production time for the "U" part, at least 12.1% for the "O" part and 33.3% for the "A" part.

Table 2 Production time in different print strategies (Unit: second)

	Our strategy	20% infill	50% infill	80% infill
"U" part	2940	3180	3897	4562
"O" part	1740	1981	2283	2520
"A" part	3001	4549	5041	5584

5.3. Energy consumption

The working principle of the printer used in this study is by extruding molten material through a nozzle, and depositing it onto a substrate layer by layer. The molten material is extruded at the set print temperature from inside the nozzle, before subsequent solidification. Cooling fans are used for speeding up the solidification process of printed material and for cooling the print nozzle when necessary. The movement of print nozzle is controlled by three motors, and a fourth motor is needed for pushing the raw filament feedstock into the print nozzle. Therefore, during a printing process, there are four motors, one heater for heating nozzle, two cooling fans and one LED display screen that will consume energy. Hence, the energy model for this printer is given as:

$$E_{total} = E_{heater} + E_{motors} + E_{screen} + E_{cooling\ fans} \tag{4}$$

where E_{heater} is the energy consumed by the heater, E_{motors} is the energy consumed by the motors, E_{screen} is the energy consumed by the LED screen and $E_{cooling\ fans}$ is the energy consumed by cooling fans during the whole fabrication process.

The average power of motors of this printer is 5.0 W, cooling fan for nozzle is 1.1 W, cooling fan for printed material is 1.08 W, heater is 60 W and the LED screen is 2.7 W, respectively. This gives a total average power consumption during printing of 69.88 W. Hence, the energy consumption of these parts can be therefore be estimated using this figure and the printing time, as shown in Table 3. As can be seen from this table, the energy savings can reach at 12.1 %, 23.7 % and 30.9 %, respectively, for the "O" part. The energy consumption of "A" part can be reduced to 254.6 kJ.

Table 3 Energy consumption in different print strategies (Unit: kJ)

	Our strategy	20% infill	50% infill	80% infill
"U" part	249.5	269.9	331.0	387.1
"O" part	147.7	168.1	193.5	213.9
"A" part	254.6	382.0	427.8	473.6

6. Conclusions and future works

In this paper, a new support generation strategy that considers both interior and exterior support via process planning to reduce the total amount of material consumption, production time and

energy consumption has been proposed. The characteristics of LPBL and PTOA are fully considered for reducing the support usage. Effect of print path strategy on support usage is considered and optimized. In addition, optimization of print orientation is also considered in the proposed algorithm for further reducing material usage. Lastly, "U", "O" and "A" parts are fabricated to verify the proposed strategy by comparing them with pre-existing generic methods. The results show that the proposed strategy can considerably reduce material consumption, production time and energy consumption, enabling AM to be a more environmentally friendly and sustainable manufacturing technique.

However, as the strategy is optimized from an efficiency and environmental perspective, the proposed strategy cannot guarantee the mechanical strength of the fabricated parts due to the least material consumption. Currently, the proposed strategy can be used for printing products without significant mechanical requirements. In future research, the mechanical requirements of products will be taken into account for optimizing AM processes.

Acknowledgements

Helps from the engineering librarians at the University of Auckland are highly appreciated. The authors are also grateful for the advice from Laboratory for Industry 4.0 and Smart Manufacturing Systems members.

References

[1] ASTM International, F2792-12a - Standard Terminology for Additive Manufacturing Technologies, 2013. doi:10.1520/F2792-12A.2.

[2] P. Zheng, Y. Wang, X. Xu, S.Q. Xie, A weighted rough set based fuzzy axiomatic design approach for the selection of AM processes, The International Journal of Advanced Manufacturing Technology. 91 (2017) 1977–1990. doi:10.1007/s00170-016-9890-8.

[3] J.S. Panchagnula, S. Simhambhatla, Manufacture of complex thin-walled metallic objects using weld-deposition based additive manufacturing, Robotics and Computer-Integrated Manufacturing. 49 (2018) 194–203. doi:10.1016/j.rcim.2017.06.003.

[4] Y. Tang, K. Mak, Y.F. Zhao, A framework to reduce product environmental impact through design optimization for additive manufacturing, Journal of Cleaner Production. 137 (2016) 1560–1572. doi:10.1016/j.jclepro.2016.06.037.

[5] J. Jiang, G. Hu, X. Li, X. Xu, P. Zheng, J. Stringer, Analysis and prediction of printable bridge length in fused deposition modelling based on back propagation neural network, Virtual and Physical Prototyping. (2019). doi:10.1080/17452759.2019.1576010.

[6] C.A. Griffiths, J. Howarth, G. De Almeida-Rowbotham, A. Rees, R. Kerton, A design of experiments approach for the optimisation of energy and waste during the production of parts manufactured by 3D printing, Journal of Cleaner

Production. 139 (2016) 74–85. doi:10.1016/j.jclepro.2016.07.182.
[7] R. Song, C. Telenko, Material and energy loss due to human and machine error in commercial FDM printers, Journal of Cleaner Production. (2017). doi:10.1016/j.jclepro.2017.01.171.
[8] J. Jiang, X. Xu, J. Stringer, Support Structures for Additive Manufacturing: A Review, Journal of Manufacturing and Materials Processing, 2 (2018) 64. doi:10.3390/JMMP2040064.
[9] J. Liu, A.T. Gaynor, S. Chen, Z. Kang, K. Suresh, A. Takezawa, L. Li, J. Kato, J. Tang, C.C.L. Wang, L. Cheng, X. Liang, A.C. To, Current and future trends in topology optimization for additive manufacturing, Structural and Multidisciplinary Optimization. 57 (2018) 2457–2483. doi:10.1007/s00158-018-1994-3.
[10] J. Liu, Y. Ma, A.J. Qureshi, R. Ahmad, Light-weight shape and topology optimization with hybrid deposition path planning for FDM parts, The International Journal of Advanced Manufacturing Technology. 97 (2018) 1123–1135. doi:10.1007/s00170-018-1955-4.
[11] A. Armillotta, M. Bellotti, M. Cavallaro, Warpage of FDM parts: Experimental tests and analytic model, Robotics and Computer-Integrated Manufacturing. 50 (2018) 140–152. doi:10.1016/J.RCIM.2017.09.007.
[12] H. ming Zhao, Y. He, J. zhong Fu, J. jiang Qiu, Inclined layer printing for fused deposition modeling without assisted supporting structure, Robotics and Computer-Integrated Manufacturing. 51 (2018) 1–13.
[13] J. Jiang, J. Stringer, X. Xu, P. Zheng, A benchmarking part for evaluating and comparing support structures of additive manufacturing, in: 3rd International Conference on Progress in Additive Manufacturing (Pro-AM 2018), 2018: pp. 196–202. doi:10.25341/D42G6H.
[14] J. Liu, A.C. To, Deposition path planning-integrated structural topology optimization for 3D additive manufacturing subject to self-support constraint, Computer-Aided Design. 91 (2017) 27–45. doi:10.1016/J.CAD.2017.05.003.
[15] J. Jiang, X. Xu, J. Stringer, A new support strategy for reducing waste in additive manufacturing, in: The 48th International Conference on Computers and Industrial Engineering (CIE 48), Auckland, 2018: pp. 1–7.
[16] M. Wang, H. Zhang, Q. Hu, D. Liu, H. Lammer, Research and implementation of a non-supporting 3D printing method based on 5-axis dynamic slice algorithm, Robotics and Computer-Integrated Manufacturing. 57 (2019) 496–505. doi:10.1016/J.RCIM.2019.01.007.
[17] Y. Ding, R. Dwivedi, R. Kovacevic, Process planning for 8-axis robotized laser-based direct metal deposition system: A case on building revolved part, Robotics and Computer-Integrated Manufacturing. 44 (2017) 67–76. doi:10.1016/j.rcim.2016.08.008.
[18] D. Frank, G. Fadel, Expert system-based selection of the preferred direction of build for rapid prototyping processes, Journal of Intelligent Manufacturing. 6 (1995) 339–345. doi:10.1007/BF00124677.
[19] D.T. Pham, S.S. Dimov, R.S. Gault, Part orientation in stereolithography, International Journal of Advanced Manufacturing Technology. 15 (1999) 674–682. doi:10.1007/s001700050118.
[20] P. Das, K. Mhapsekar, S. Chowdhury, R. Samant, S. Anand, Selection of build orientation for optimal support structures and minimum part errors in additive manufacturing, Computer-Aided Design and Applications. (2017) 1–13. doi:10.1080/16864360.2017.1308074.
[21] H.D. Morgan, J.A. Cherry, S. Jonnalagadda, D. Ewing, J. Sienz, Part orientation

optimisation for the additive layer manufacture of metal components, The International Journal of Advanced Manufacturing Technology. 86 (2016) 1679–1687. doi:10.1007/s00170-015-8151-6.
[22] J. Jiang, X. Xu, J. Stringer, Optimisation of multi-part production in additive manufacturing for reducing support waste, Virtual and Physical Prototyping. (2019) 1–10. doi:10.1080/17452759.2019.1585555.
[23] Y. Jin, J. Du, Y. He, Optimization of process planning for reducing material consumption in additive manufacturing, Journal of Manufacturing Systems. 44 (2017) 65–78. doi:10.1016/J.JMSY.2017.05.003.
[24] J. Lee, K. Lee, Block-based inner support structure generation algorithm for 3D printing using fused deposition modeling, The International Journal of Advanced Manufacturing Technology. 89 (2017) 2151–2163. doi:10.1007/s00170-016-9239-3.
[25] L. Lu, A. Sharf, H.S. Zhao, Y. Wei, Q.N. Fan, X.L. Chen, Y. Savoye, C.H. Tu, D. Cohen-Or, B.Q. Chen, Build-to-Last: Strength to Weight 3D Printed Objects, Acm Transactions on Graphics. 33 (2014) 1–10. doi:Artn 97\r10.1145/2601097.2601168.
[26] T. Lee, J. Lee, K. Lee, Extended block based infill generation, The International Journal of Advanced Manufacturing Technology. 93 (2017) 1415–1430. doi:10.1007/s00170-017-0572-y.
[27] R. Mertens, S. Clijsters, K. Kempen, J.-P. Kruth, Optimization of Scan Strategies in Selective Laser Melting of Aluminum Parts With Downfacing Areas, Journal of Manufacturing Science and Engineering. 136 (2014) 061012. doi:10.1115/1.4028620.
[28] D. Wang, S. Mai, D. Xiao, Y. Yang, Surface quality of the curved overhanging structure manufactured from 316-L stainless steel by SLM, International Journal of Advanced Manufacturing Technology. 86 (2016) 781–792. doi:10.1007/s00170-015-8216-6.
[29] J. Jiang, J. Stringer, X. Xu, R.Y. Zhong, Investigation of printable threshold overhang angle in extrusion-based additive manufacturing for reducing support waste, International Journal of Computer Integrated Manufacturing. 31 (2018) 961–969. doi:10.1080/0951192X.2018.1466398.
[30] F. Decuir, K. Phelan, B.C. Hollins, Mechanical Strength of 3-D Printed Filaments, in: 2016 32nd Southern Biomedical Engineering Conference (SBEC), IEEE, 2016: pp. 47–48. doi:10.1109/SBEC.2016.101.
[31] J. Jiang, J. Lou, G. Hu, Effect of Support on Printed Properties in Fused Deposition Modelling Processes, Virtual and Physical Prototyping. (2019). doi:10.1080/17452759.2019.1568835.
[32] J. Jiang, J. Stringer, X. Xu, Support Optimization for Flat Features via Path Planning in Additive Manufacturing, 3D Printing and Additive Manufacturing. (2018). doi:10.1089/3dp.2017.0124.